Europe and Scandinavia during most periods of May–August 2018, accompanied with an eastward shifting Greenlandic low pressure system and a northward shifting jet stream. Such atmospheric circulation anomalies brought extremely warm and sunny weather over the Baltic Sea during summer 2018 and high surface solar radiation. It is found that MHW duration is significantly correlated with surface air temperature anomaly, which is caused by the anomalous atmospheric circulation patterns. The results also suggest that, among all atmospheric surface heat flux components, the very high positive anomaly of the surface solar radiation is the primary contributor to the extremely warm surface water in the Baltic Sea in summer 2018.

Acknowledgements

It is acknowledged that Jacob L. Høyer at Danish Meteorological Institute has kindly provided the complete dataset of Level 4 SST for this study.

Section 4.5. Space-based observations of surface signatures in the wake of the 2018 Eastern Pacific tropical cyclones

Authors: Clément Combot, Yves Quilfen, Alexis Mouche, Jérôme Gourrion, Clément de Boyer Montégut, Bertrand Chapron, Jean Tournadre.

Statement of main outcome: In this section, a new focus is given on the ocean response induced by Tropical Cyclones. Tropical Cyclones are among the most devastating and destructive natural hazards. Unfortunately, predicting the intensity and evolution of such individual event is still extremely difficult, owing to various internal and environmental factors, including interactions with the ocean interior. In that context, multiple satellite remote sensing observations are essential, and today, combined with denser ARGO interior measurements, the upper ocean responses to moving tropical cyclones can be more efficiently captured and monitored.

Ref No.	Product name & type	Documentation
4.5.1	SST_GLO_SST_L4_NRT_OBSERVATIONS_010_001	PUM: https://marine.copernicus.eu/documents/PUM/CMEMS-SST-PUM-010-001.pdf QUID: https://resources.marine.copernicus.eu/documents/QUID/CMEMS-OSI-QUID-010-001.pdf
4.5.2	SEALEVEL_GLO_PHY_L3_NRT_OBSERVATIONS_008_044	PUM: https://marine.copernicus.eu/documents/PUM/CMEMS-SL-PUM-008-032-062.pdf QUID: https://marine.copernicus.eu/documents/QUID/CMEMS-SL-QUID-008-032-062.pdf
4.5.3	INSITU_GLO_TS_NRT_OBSERVATIONS_013_001_B	PUM: https://marine.copernicus.eu/documents/PUM/CMEMS-INS-PUM-013.pdf QUID: https://resources.marine.copernicus.eu/documents/QUID/CMEMS-INS-QUID-013.pdf
4.5.4	Non-CMEMS product: ISAS13-clim Monthly climatology of temperature and salinity profile used as a background stratification information, in case of argo absence. Developed by F.Gaillard & al 2016 (LOPS/IFREMER).	Downloaded from: https://www.seanoe.org/data/00348/45945/ Reference paper: https://journals.ametsoc.org/doi/pdf/10.1175/JCLI-D-15-0028.1
4.5.5	Non-CMEMS product: IBTrACS Best-tracks are post-storm analyses at every 6-hours of Tropical and subtropical cyclones, giving several characteristic parameters (position, intensity,size) . They are produced by several dedicated centres and gathered in a homogeneous database named IBTrACS: International Best Track Archive for Climate Stewardship.	Downloaded from: https://www.ncdc.noaa.gov/ibtracs/index.php?name=ibtracs-data-access User Manual: ftp://eclipse.ncdc.noaa.gov/pub/ibtracs/v04r00/doc/IBTrACS_v04_column_documentation.pdf Quality information: https://journals.ametsoc.org/doi/pdf/10.1175/2009BAMS2755.1
4.5.6	Non-CMEMS product: SAR-Sentinel-1A/B wind field: C-band radar with high resolution and dual polarisation (Co- & Cross- pol) signal. The wind product used was retrieved by the inversion scheme published by Mouche & al 2017 (LOPS/IFREMER) from L1 sigma0 of ESA Copernicus. Data were collected in the context of ESA's SHOC campaign. (SHOC: Satellite Hurricane Observations Campaign).	- ESA Copernicus L1 sigma0: Copernicus open access hub (https://scihub.copernicus.eu/) and Sentinel-1 Mission Performance Center (MPC S-1) - SAR's Tropical Cyclone Wind Product: (Distribution site to come soon) Contact: alexis.mouche@ifremer.fr

4.5.1. Introduction

Over the Eastern Pacific region, 2018 has been a very active Tropical Cyclone season. The accumulated cyclone energy reaches a record value of 316.10^4 kt^2 (NOAA, Annual 2018 report; Kruk and Schreck 2019). As shown in the background of Figure 4.5.1a, a persistent positive Sea Surface Temperature Anomaly (SSTA) up to 1.5°C extended over the entire region, to explain this very active 2018 season in combination with an enhanced convection (Kruk and Schreck 2019).

Associated to the extreme wind forcing conditions, distinctive localised impacts have long been attracting considerable attention. Indeed, quite systematically, a tropical cyclone will leave persistent signatures in its

wake (Leipper 1967; Price 1981). The vigorous induced mixing and resulting intense upwelling generally cool the upper ocean mixed layer, stirring warm surface waters with colder waters below (Ginis 2002). Consequently, a tropical cyclone wake is generally characterised by a surface cold anomaly, possibly accompanied with nutrient blooms. Moreover, governed by intense isopycnal displacements (Geisler 1970), a tropical cyclone can also leave prominent sea-surface height anomalies in its wake. Resulting surface depressions can reach 0.3–0.5 m, depending upon the forcing intensity, size, translation speed, and ocean stratification conditions (Kudryavtsev et al. 2019a). Building on the actual satellite altimeter constellation (presently up to 6 satellites are available), satellite sea surface height estimates may more likely cross such trenches. Using both sea surface height and temperature observation, a more consistent view of the tropical cyclone characteristics can thus be obtained with additional support of a semi-empirical 2D model to interpret the oceanic answer. Here, the wakes of seven Eastern Pacific tropical systems are presented. To illustrate and further discuss the influence of the forcing parameters, the analysis mainly focuses on three particular major tropical cyclones: Hector (August), Lane (August) and Sergio (October). Hector experienced two intensification periods with maximum winds over 110 kt that lasted up to 7 days (NHC archive). Lane was the second wettest storm in USA territory with 1341 mm accumulated rainfall (NHC archive). Finally, Sergio left a particularly deep ocean signature (Figure 4.5.1). Above all, these three tropical cyclones are relevant cases as they benefit from longer time monitoring by satellites.

4.5.2. Data analysis

A database has been set up that merges satellite observations, from altimeters, radiometers, and high-

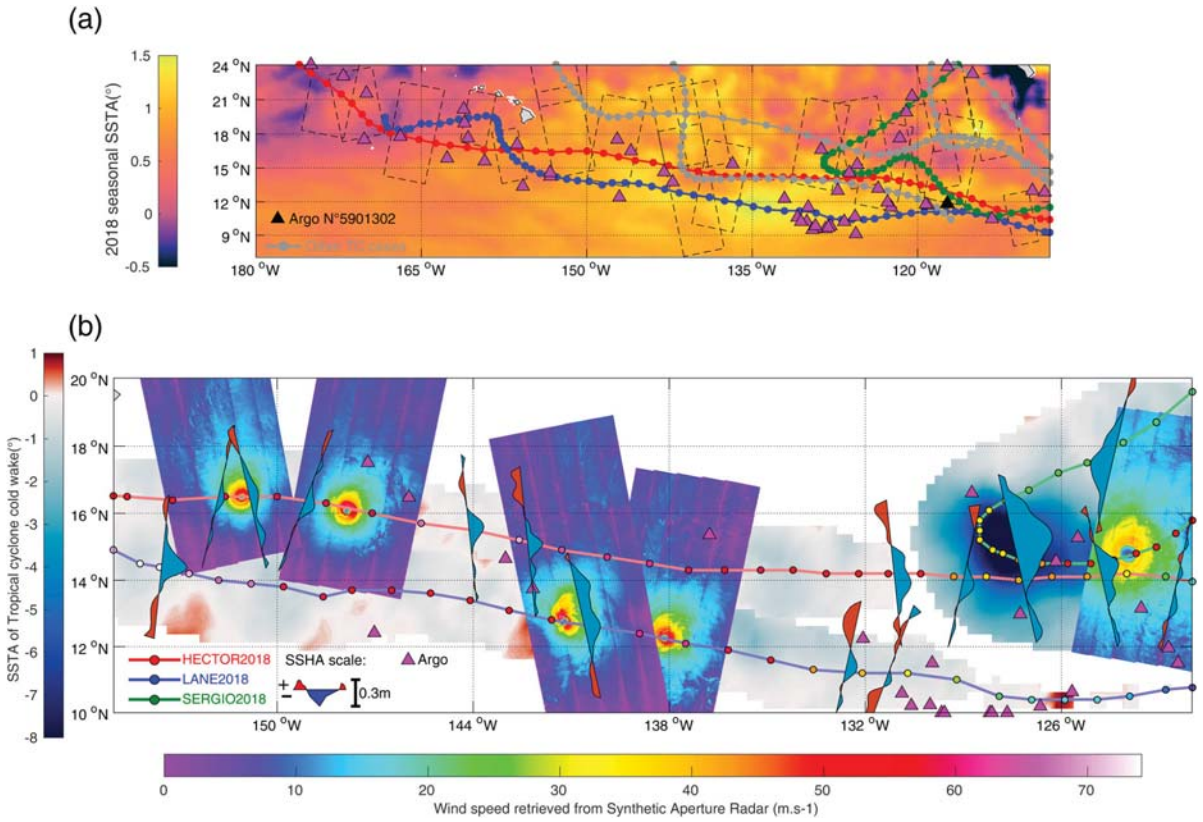

Figure 4.5.1. Constellation of satellite (product ref 4.5.1 & 4.5.2) and in-situ observations (product ref 4.5.3 & 4.5.4) for wake analysis over Eastern Pacific in 2018. (a) Overview of the database with all the tracks (coloured lines), SAR swaths (dashed contours) and Argo floats (magenta triangles) represented. The background field depicts the 2018 seasonal thermal anomalies (globally positive). (b) A zoom on Hector, Lane and Sergio. The 3 tropical cyclones wakes are represented by shaded areas for SSTA (see colorbar) as well as for SSHA anomalies (blue = negative, red = positive). Specific Sentinel 1A/B swaths were selected to map the tropical cyclone wind fields (product ref. 4.5.6). To clarify, not all the altimetry and SAR crossings available for the 3 tropical cyclones are displayed. Best-track information were added as the synoptic positions and intensities (coloured circles, product ref 4.5.5), with Hector and Lane heading westward and Sergio drawing a loop that ends northeast.

resolution Synthetic Aperture Radars (SAR), with Argo float data. The 6-hour Best-Track data set further provides several parameters over the tropical cyclone life such as position, intensity and specific wind radii (Product ref. 4.5.5). For each track, all available altimeter observations from the L3 CMEMS products were assembled for the different storm positions (Figure 4.5.1, product ref. 4.5.2), keeping only altimeter passes crossing the tropical cyclone wake afterwards. The well-defined trough left behind the tropical cyclones (blue shaded areas on the altimetry tracks in Figure 4.5.1) was used to directly estimate the sea surface height anomaly, i.e. the maximum difference between the bottom and the top of the altimeter sea surface height profile. As the tropical cyclone generates near-inertial oscillations (Geisler 1970), the altimeter may not sample the maximum trough value. For each Best-Track synoptic time, we thus kept the largest sea surface height anomalies among all the closest time/space colocated altimeter passes. When only one altimeter pass is available, the unique anomaly estimate was kept. This can thus introduce a slight underestimation of the altimeter trough.

The daily CMEMS L4 sea surface temperature product is used to estimate the thermal anomalies at each Best-Track synoptic position (product ref. 4.5.1). The cold wake intensity was estimated as the difference between a 2-week average of pre-storm sea surface temperature conditions and the daily post-storm sea surface temperature field. In case of pre-existing storms or loop trajectory, this pre-storm time window was reduced to withdraw the cooling of previous forcing. Shaded areas in Figure 4.5.1b trace the maximum cooling, from 1 to 3 days after the Best-Track synoptic time (Dare and McBride 2011; Vincent et al. 2012). Finally, using wind radii information from Best-Track, all Argo data inside the 34 kt wind radius were selected to infer the ocean stratification parameters (magenta triangles in Figure 4.5.1, product ref 4.5.3). From the nearest profile, we extracted the Brunt-Väisälä frequency N in the thermocline (Figure 4.5.2c), known to strongly influence the oceanic response to tropical cyclone forcing (Reul et al. 2014). In absence of Argo floats, the ISAS-13 climatology was used (product ref 4.5.4). As obtained in Figure 4.5.1b, rather moderate signatures are found for Hector and Lane, with maximum thermal and height anomalies amplitude of −1.7° and −0.17 m, respectively. A stronger cooling and a deeper trough are found for Sergio, with respective signatures larger than −7°C and −0.3 m. The first two cyclone cases were small intense storms with fast translation speed (V_{fm} = 7 m s^{-1}), while Sergio had a weaker wind intensity but is a large and slowly moving cyclone (V_{fm} = 4 m s^{-1}). As anticipated, the overall tropical cyclone induced-stirring process depends on its intensity, but also on its size and translation speed (Reul et al. 2014; Kudryavtsev et al. 2019a). The tropical cyclone wind structure is therefore of paramount importance, and the Best-Track data may not be precise enough to depict it, especially the determination of the maximum wind radius (R_{max}) can be subject to large errors (Kossin et al. 2007; Knaff et al. 2015).

To overcome such a limitation, SAR measurements have therefore been used (product ref. 4.5.6), which can provide unique observations of high resolution wind patterns in tropical cyclones (Mouche et al. 2019). As collected, 1-km resolution data from Copernicus/ESA's Sentinel 1A/B operating in C-band and VH cross-polarisation provide reliable surface winds up to 70 m s^{-1} (Mouche et al. 2017; Mouche et al. 2019). A total of 23 SAR scenes were collected with maximum winds ranging from 25 to 70 m s^{-1} (Figure 4.5.2a), representing small to medium size systems (Figure 4.5.2b). For each SAR scene, an objective analysis was used to determine the centre of the storm and to extract the maximum wind speed (Vmax) and radius of maximum wind information (Combot et al. 2020). These estimates are compared to the Best-Track ones in Figures 4.5.2a, b. An excellent consistency is found for the maximum wind speed parameter, with a correlation coefficient of 0.95, a very weak normalised bias, and a root mean square difference of about 4 m s^{-1}, that is partly associated with the discretization of the Best-Track estimates. For the radius of maximum winds, the correlation is significantly lower but still high (0.80). Yet, compared to Best-Track values, SAR estimates are not discrete and therefore more likely to provide accurate values for small size TCs (Rmax < 30 km, Combot et al. 2020).

Pre-storm ocean stratification and heat content are key variables that determine ocean/atmosphere feedback mechanisms and the associated evolution of tropical cyclones. The lower panels in Figure 4.5.2 show the temperature, salinity and density profiles measured by an Argo float a few days before (~7 days, in blue) and after (~3 days, in magenta) Sergio's passage in category 4 at that time. The corresponding ISAS profiles are also displayed for the two climatological months close to the Argo profile time (black lines). As obtained from the pre-storm Argo profile, the ocean stratification was much stronger than the climatological values (values indicated in the lower right panel), mainly due to a 30-m thick surface layer much fresher than usual, which is confirmed by the surrounding floats. As a result, mixing and associated salinity and temperature anomalies are reduced, and the

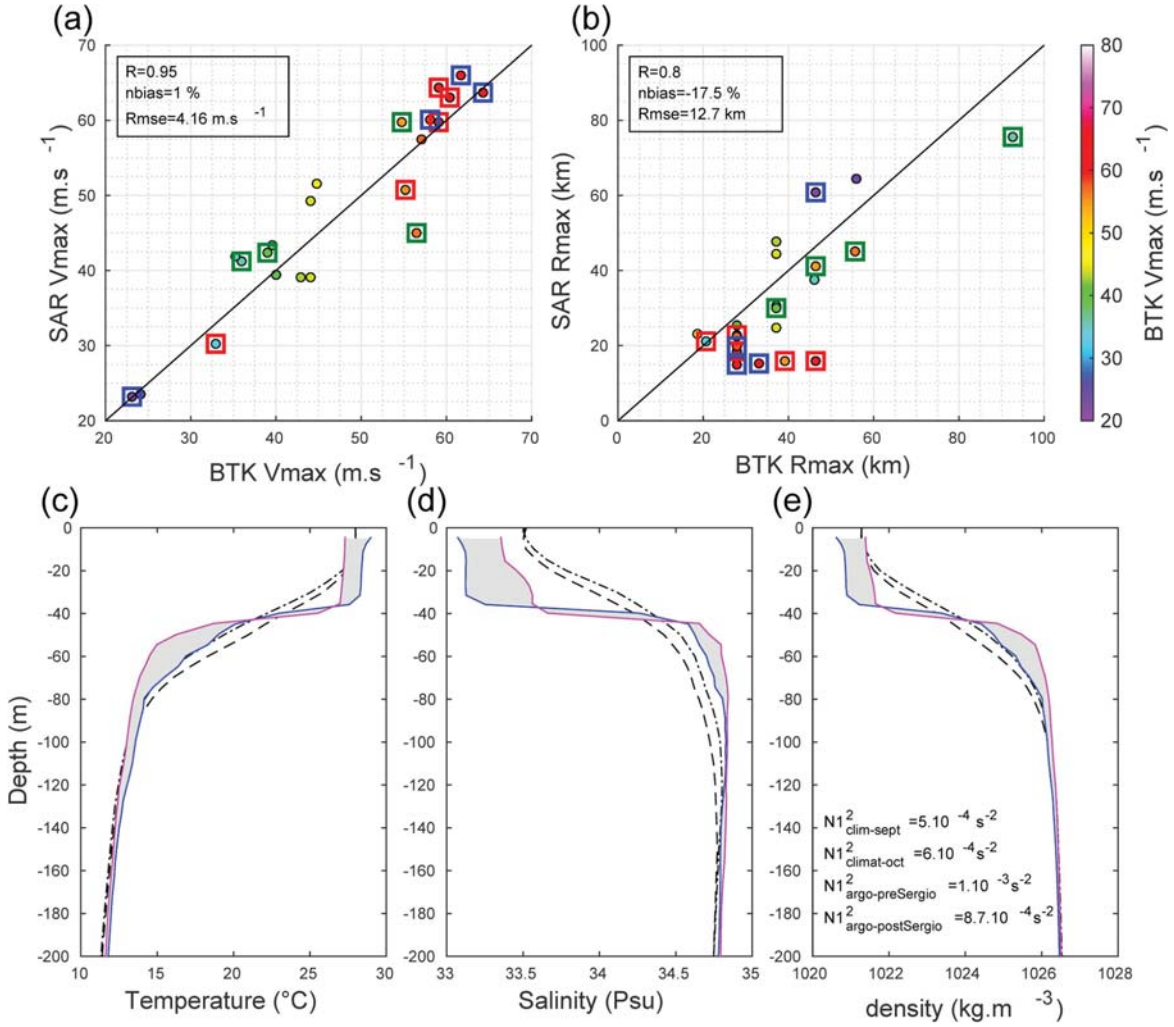

Figure 4.5.2. Upper panel: Comparison between Best-Track (product ref 4.5.5) and SAR (product ref 4.5.6). Maximum wind speed (a) and radius of maximum wind speed (b) with dots coloured as a function of Vmax. Following the Figure 4.5.1 convention, the three particular TCs dots are notified with coloured squares, red = Hector, blue = Lane, green = Sergio. Lower panel: Profiles of temperature (c), salinity (d) and density (e) of Argo and ISAS climatology (product ref 4.5.3 & 4.5.4) at the Sergio's location on 3rd October 2018 at 13h40, when it was particularly strong (~60 m s^{-1}). The two surrounding months, September (dashed line) and October (dashed dotted line), from the ISAS climatology profiles are shown. Two Argo profiles were selected, one before (26th September 2018 in blue) and one after (6th October 2018 in magenta) the Sergio path. Shaded areas illustrate the anomalies left by Sergio, a slight deepening (~10 m) and cooling (~2°C) of the mixed layer are observed. These profiles were acquired near 117 °W and 12 °N (black triangle in Figure 4.5.1.a, profiler number: 5901302).

stratification remains very strong during and after Sergio's passage which is an important limiting factor for oceanic feedback on tropical cyclones evolution.

4.5.3. Analysis from a semi-empirical model

Following Geisler (1970) and Price (1981), Kudryavtsev et al. (2019a) proposed a semi-empirical framework to jointly analyse and interpret tropical cyclones sea surface temperature and height anomalies. It is assumed that the ocean response to a moving TC is largely dominated by baroclinic effects. Considering this assumption, scaling laws issued from the semi-empirical modelling approach developed by Kudryavtsev et al. (2019) can be expressed as

$$\frac{SSTA}{V_{\max} \cdot N^{(3/2)}/(g \cdot \alpha \cdot f^{(1/2)})} \propto \left(\frac{V_{fm}}{f \cdot R_{\max}}\right)^{-1} \quad (1)$$

$$\frac{g.SSHA}{V_{\max}^2} \propto \frac{R_{\max}.N}{V_{fm}} \quad (2)$$

with f, the Coriolis parameter, V_{fm} the translation speed, α the thermal expansion coefficient, g the gravitational acceleration on Earth, and N the Brunt-Väisälä

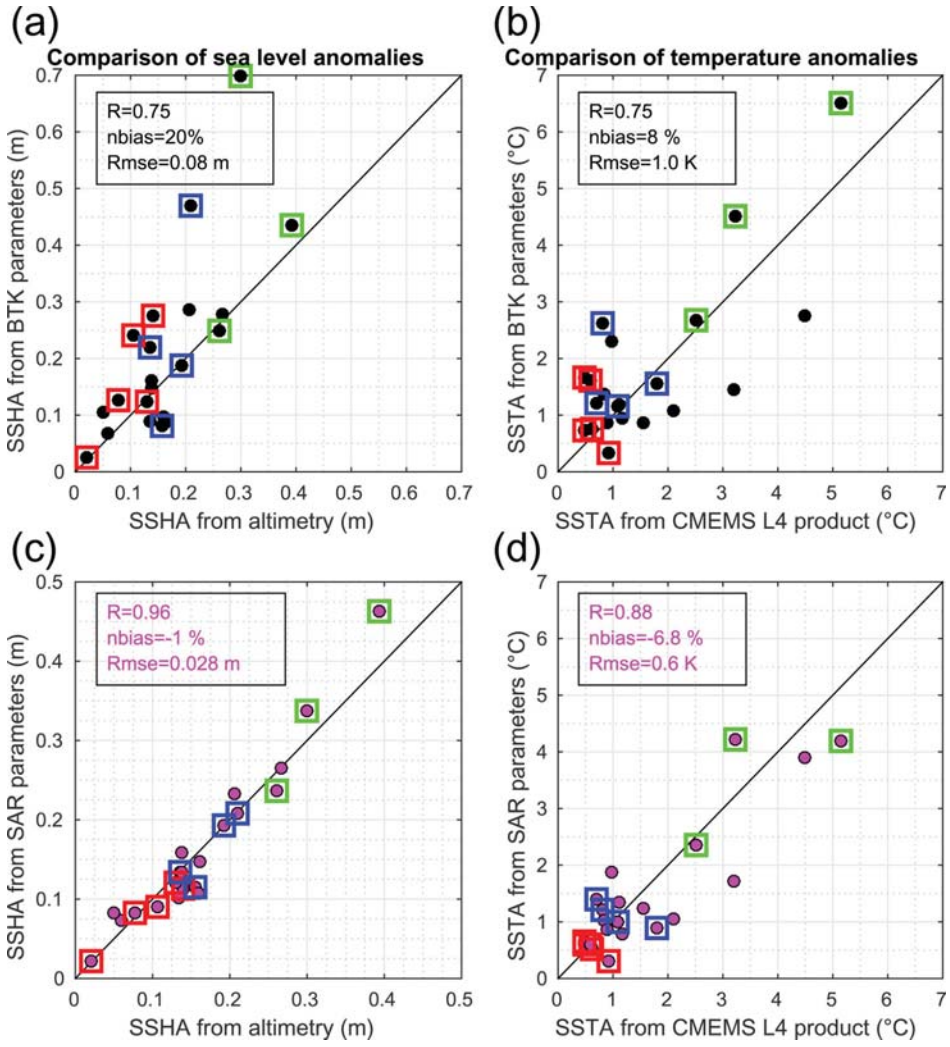

Figure 4.5.3. Comparison of Sea Surface Height (left column, product ref 4.5.2) and Sea Surface Temperature (right column, product ref 4.5.3) anomalies between satellite measurements (*x*-axis) and estimation from the semi-empirical model (*y*-axis): (a) and (b) represent the estimates inferred from Best-Track information (product ref 4.5.5); (c) and (d) from SAR-derived wind field (product ref 4.5.6). The 3 reference cases are reported according to the same convention than in Figure 4.5.2. The required spatial collocation between SAR and altimetry has slightly reduced the numbers of points (21) as used for Figure 4.5.2(a,b).

frequency. Best-Track and SAR offer two different sets of Vmax/Rmax estimates, giving different semi-empirical predictions that are compared in Figure 4.5.3. Overall, the results agree well with large correlation between observations and predictions ($R \geq 0.75$). These correlation coefficients are significant at the 95% confidence level but, due to the rather small sample size, this cannot be accurately assessed. However, ongoing research confirms these findings with a much larger sample size including $N > 100$ SAR scenes colocated with TCs for the recent years and over all the ocean basins. Bringing improved high-resolution description within the maximum wind region, SAR estimates give a significantly closer agreement with the proposed scaling laws ($R \geq 0.88$). The Hector case (red squares) remarkably illustrates the improvement, as large maximum wind radius discrepancies were indeed observed between the two data sources (Figure 4.5.2b). As also shown in Figure 4.5.3, the Sergio case highlights a larger dynamical range for its wake signature, going from 2.5°C to 5.2°C cooling and from 0.26 to 0.39 m sea level drop. This overall stronger induced oceanic answer arises from its larger size and lower translation speed and is well accounted for by the semi-empirical model when fed by the SAR observations. This is particularly true with regard to the two points departing the most from the 1:1 line, Sergio and Lane (Figure 4.5.3a), for which overestimation of Best-Tracks for maximum wind speed and its radius (Figure 4.5.2) led to unrealistic predictions of sea surface anomalies.

The proposed interpretation framework can thus guide the combined use of sea surface temperature and height amplitude changes measured in the wake of tropical cyclones. It can help to inform about the resulting strength of hurricane-induced mixing and upwelling. This opens a bottom-up approach to guide future investigations to help document the resulting wind forcing and practical drag coefficient under extreme tropical cyclone conditions (Kudryavtsev et al. 2019a, 2019b).

4.5.4. Summary

This study highlights the use of multi-platform observations for the analysis of tropical cyclones and their induced oceanic answer. As a main outcome, it is shown that the combination of low and high resolution satellite sensors are of paramount importance to better depict and monitor the tropical cyclones wind patterns, and to interpret the air/sea coupling that imprints the cyclone wake. In particular the study shows that altimeter and SAR measurements can provide unique information to help analysis and monitoring of extreme events. The wide-swath altimetry SWOT mission foreseen in 2021 will be a unique opportunity for further research and applications, notably since it will provide a 2D mapping of sea level anomalies left by tropical cyclones.

Acknowledgements

This work was supported by CNES TOSCA program (COWS and SILLAGE projects), by the European Space Agency through S1-4SCI Ocean Study project (contract 4000115170/15/I-SBo), Sentinel-1 A Mission Performance Center (contract4000107360/12/I-LG), EUMETSAT CHEF project, ANR (FEM) CARAVELE project.

Section 4.6. Record wave storm in the Gulf of Cadiz over the past 20 years and its impact on harbours

Authors: Marta de Alfonso, José María García-Valdecasas, Roland Aznar, Begoña Pérez-Gómez, Pablo Rodríguez, Francisco Javier de los Santos and Enrique Álvarez-Fanjul

Statement of main outcome: The Gulf of Cadiz region suffered the most severe wave storm over the past 20 years produced by the storm Emma in March 2018. The combined effect of high waves and sea level surge aggravated the storm risk potential. The CMEMS products, the local wave and sea level forecasting systems (PORTUS system) and their associated alerts and downstream services worked properly and warnings were sent in advance to the users. Several actions were carried out to mitigate the impact of the event. For example, harbours stopped operations to prevent accidents and assure safety. The material damages were considerable but, probably due to the preventive actions, no personal damages were suffered.

CMEMS products used

Ref. No.	Product name & type	Documentation
4.6.1	INSITU_IBI_TS_REP_OBSERVATIONS_013_040 Observations reprocessed	PUM: https://marine.copernicus.eu/documents/PUM/CMEMS-INS-PUM-013.pdf QUID: https://marine.copernicus.eu/documents/QUID/CMEMS-INS-QUID-013-040.pdf
4.6.2	INSITU_IBI_NRT_OBSERVATIONS_013_033 Observations	PUM: https://marine.copernicus.eu/documents/PUM/CMEMS-INS-PUM-013.pdf QUID: https://marine.copernicus.eu/documents/QUID/CMEMS-INS-QUID-013-030-036.pdf
4.6.3	INSITU_GLO_WAVE_REP_OBSERVATIONS_013_045 Observations reprocessed	PUM: https://marine.copernicus.eu/documents/PUM/CMEMS-INS-PUM-013.pdf QUID: https://marine.copernicus.eu/documents/QUID/CMEMS-INS-QUID-013-045.pdf
4.6.4	IBI_ANALYSIS_FORECAST_WAV_005_005 Model analysis and forecast	PUM: https://marine.copernicus.eu/documents/PUM/CMEMS-IBI-PUM-005-005.pdf QUID: https://marine.copernicus.eu/documents/QUID/CMEMS-IBI-QUID-005-005.pdf
4.6.5	IBI_REANALYSIS_WAV_005_006 Model reanalysis	PUM: https://marine.copernicus.eu/documents/PUM/CMEMS-IBI-PUM-005-006.pdf QUID: https://marine.copernicus.eu/documents/QUID/CMEMS-IBI-QUID-005-006.pdf
4.6.6	PORTUS coastal and local wave forecast in the Gulf of Cadiz (non CMEMS product)	URL: https://www.puertos.es/en-us/oceanografia/Pages/portus.aspx OPeNDAP: https://opendap.puertos.es
4.6.7	PORTUS sea level/storm surge forecasting system (NIVMAR-ENSURF) (non CMEMS product)	URL: https://www.puertos.es/en-us/oceanografia/Pages/portus.aspx. OPeNDAP: https://opendap.puertos.es
4.6.8	Puertos del Estado downstream SAMOA/CMA services for Port Authorities (non CMEMS product)	URL: https://cma.puertos.es/ OPeNDAP: https://opendap.puertos.es

4.6.1. Introduction

During February-March 2018 several storms including Emma, affected the maritime area in the south of Europe. In particular, Emma was characterised by an area of deep low pressure located west of the Iberian Peninsula, channelling strong southwesterly winds over the Gulf of Cadiz, and generating the highest significant wave heights recorded in the region. The impact of these huge waves in the coastal infrastructures was strengthened by less extreme, but still important, sea level and surge. In this paper, this event is studied employing data from the PORTUS system (Product refs: 4.6.6 and